PHYSICAL REVIEW A VOLUME 24, NUMBER 2 AUGUST 1981

Dielectronic recombination rate for Mo^{31+}

K. J. LaGattuta and Yukap Hahn
Physics Department, University of Connecticut, Storrs, Connecticut 06268
(Received 29 September 1980)

A detailed calculation of the dielectronic recombination (DR) rate coefficient is presented for the system $Mo^{31+} + e^-$, in which the initial states of the ion are $i_1 = 1s^2\,2s^2\,2p^6\,3s$, $i_2 = 1s^2\,2s^2\,2p^6\,3p$, and $i_3 = 1s^2\,2s^2\,2p^6\,3d$. All possible intermediate autoionizing states and their cascade decays are included. The necessary Auger and radiative transition probabilities are computed using nonrelativistic Hartree-Fock wave functions. Various angular-momentum-averaging schemes are examined, and a simple and general procedure applicable to all open- and closed-shell targets is developed. In this, the orbital and spin angular momenta of the Auger-active electron pair is held fixed while all other angular momenta are averaged. As expected, the main contribution to the DR rate comes from the excitation of $2p$ electrons (a $\Delta n \neq 0$ process). The overall DR rates for $i = i_2$ and $i = i_3$ are $\sim 30\%$ less than the rate for $i = i_1$. The overall DR rate for $i = i_1$ is slightly greater, at 3 keV, than the rate for the ion Mo^{32+}.

I. INTRODUCTION

A. General

We report the results of a detailed calculation of the dielectronic recombination (DR) rate coefficient for the ion Mo^{31+} (Na-like Mo) over a range of temperatures of several keV, centered at 3 keV. The invoked procedures are similar to those of Gau and Hahn.[1] It is now well known that accurate values of the DR rate coefficients are essential for the reliable determination of ionization equilibria in low density plasmas. Examples of these are present day tokamak plasmas and the solar corona.

In tokamaks, metal atoms are sputtered into the plasma from the container walls (iron) and from the current limiter (molybdenum).[2] The atoms, becoming partially ionized, emit line radiation. This radiation exits the (optically thin) plasma resulting in a reduction of the rate of temperature growth. At the same time, noble gas atoms may be injected into the plasma for diagnostic purposes. Measurements of the intensities of the characteristic radiations of the ions of these elements are used to deduce the free electron temperature and density. The ability to make such deductions as well as to understand the radiative losses due to impurity metal ions depends upon a precise knowledge of the ionization equilibrium and, hence, of the DR rate coefficients. (The availability of accurate rate coefficients for collisional ionization is equally important).

Because pre-1964 calculations of ionization equilibria did not include DR, solar coronal temperatures deduced from the theory of ionization balance were in disagreement with the temperatures determined from line-broadening measurements. The line-broadening measurements implied higher temperatures, suggesting either that recombination rate coefficients were too small or that ionization-rate coefficients were too large. Burgess[3] pointed out the importance of DR, i.e., its role in increasing the overall recombination rate coefficient. He emphasized the need for a careful calculation of select DR rate coefficients and then, based upon several such calculations, proposed a semiempirical formula,[4] valid for ions of $Z \lesssim 20$, and for DR rate coefficients dominated by $\Delta n = 0$ excitations. The Burgess formula was later modified by Merts *et al.*,[5] for application to the ions of slightly heavier elements and for the case $\Delta n \neq 0$. The further extension of the Burgess-Merts formula to elements heavier than Fe may now be needed. Toward this end, it will be necessary to perform precise calculations of DR rate coefficients for specific ions in the region of $Z \gtrsim 26$.

Such precise calculations of DR rate coefficients for heavy elements have begun to appear[6-8] for Mo^{38+} and Mo^{32+}. These studies employ Hartree-Fock wave functions with either nonlocal exchange[7] or a local exchange approximation.[8] This represents an improvement in technique over previous works in which the much simpler hydrogenic wave functions were used. Interestingly, however, the calculations of Refs. 7 and 8 are found to agree with the predictions of the Burgess-Merts formula for the ion Mo^{32+}. This agreement is fortuitous, as a careful consideration of the details of the various calculations shows. Thus, the calculations of Ref. 7 account for the effects of transitions to all possible doubly excited states of the ion Mo^{31+} (which increases the rate) and includes the effects of cascade (which decreases the rate). However, the calculations of Ref. 8 are restricted to the excitations $2p + kl_c \rightarrow 3snl$, $2p + kl_c \rightarrow 3dnl$, and $2s + kl_c \rightarrow 3pnl$, and do not treat cascade. That the results of these two calculations agree also

suggests that for Mo^{32+} at 1–6 keV, a subset of the optically allowed (dipole) excitations dominates the DR rate coefficient. This is one of the key assumptions made by Burgess.[3] In Secs. II and V, we bring quantitative evidence to bear upon this point. It is important to realize that the decrease in the DR rate produced by cascade tends to be canceled by the increase produced by including all of the accessible intermediate states. Whether this cancellation is nearly complete or only partially complete will depend upon the structure of the system being studied.[7]

B. Formalism

In the language of Ref. 1, the DR rate coefficient, in cm^3/sec, for the process $Mo^{31+}+e^- \rightarrow (Mo^{30+})^{**} \rightarrow (Mo^{30+})^{*}+\gamma$ is

$$\alpha_{DR}(i)=\sum_d\sum_{l_c}\alpha_{DR}(i,l_c\rightarrow d)$$
$$=\left(\frac{2\pi\,\mathrm{Ry}}{k_BT}\right)^{3/2}\alpha_0\sum_d\sum_{l_c}\exp\left(\frac{-E_c}{k_BT}\right)V_a(i,l_c\rightarrow d)\omega(d)\,, \tag{1}$$

with the fluorescence yield,

$$\omega(d)=\Gamma_r(d)/[\Gamma_a(d)+\Gamma_r(d)]\,. \tag{2}$$

In Eq. (1), l_c and E_c are the angular momentum and energy, respectively, of the continuum electron. The initial state of the ion is denoted by i and the doubly excited resonant intermediate state is labeled d. The constant $\alpha_0=2^{3/2}g^3$. The capture probability $V_a(1/\mathrm{sec})$ is related to the Auger probability $A_a(1/\mathrm{sec})$ by a statistical factor tical factor

$$V_a(i,l_c\rightarrow d)=(g_d/g_i\,g_e)A_a(d\rightarrow i,l_c)\,. \tag{3}$$

Here, g_d and g_i are the statistical weights of the states d and i and $g_e=2$ is the intrinsic statistical weight of the continuum electron. The Auger width is

$$\Gamma_a(d)=\sum_i\sum_{l_c}A_a(d\rightarrow i,l_c) \tag{4}$$

and the radiative decay width is

$$\Gamma_r(d)=\sum_f A_r(d\rightarrow f)\,, \tag{5}$$

with f specifying the final state (singly excited). In the noncascade stabilization scheme, the sum in Eq. (5) runs over all final states, whether or not they are stable to electron emission. The probability for spontaneous radiative decay is

$$A_r(d\rightarrow f)=\left(\frac{(4l_d+2-h_d)h_f}{4l_f+2}\right)\left(\frac{4k_\gamma^3}{3\tau}\right)\frac{l_>R_{fd}^2}{2l_d+1}\,. \tag{6}$$

Here, k_γ is the magnitude of the wave vector of the emitted photon, R_{fd} is the transition dipole radial matrix element, τ is the atomic unit of time ($\tau=2.42\times10^{-17}$ sec) and the angular momentum quantum numbers l_d and l_f refer to the electron making the radiative transition. $l_>$ is the greater of l_d and l_f. The number of holes in the subshell to which the transition occurs is h_f and the number of holes in the parent subshell is h_d. All quantities are in atomic units. In the coupling independent (fully angular momentum averaged) scheme the Auger probability is[9]

$$A_a(d\rightarrow i,l_c)=\left(\frac{(h_1+1)(4l_a+2-h_a)(4l_b+2-h_b)}{(4l_a+2)(4l_b+2)}\right)$$
$$\times A_a^{(0)}(d\rightarrow i,l_c) \tag{7}$$

for $\phi_a\neq\phi_b$ and

$$A_a(d\rightarrow i,l_c)=\left(\frac{(h_1+1)(4l_a+2-h_a)(4l_a+1-h_a)}{2(4l_a+2)(4l_a+1)}\right)$$
$$\times A_a^{(0)}(d\rightarrow i,l_c) \tag{8}$$

for $\phi_a=\phi_b$, where ϕ_a and ϕ_b are the single particle orbitals occupied by the (two) excited electrons in the state d, where h_1, h_a, and h_b are the number of holes in the initial state (bound) orbital and in the intermediate state orbitals, respectively, and where

$$A_a^{(0)}(d\rightarrow i,l_c)=\left(\frac{2\pi}{\tau}\right)\left(\frac{(2l_1+1)(2l_c+1)(2l_a+1)(2l_b+1)}{4l_1+2}\right)$$
$$\times\sum_f\sum_g(2f+1)(2g+1)|I(f,g)|^2\,. \tag{9}$$

In Eq. (9), τ is the atomic unit of time and $I(f,g)$ is the Auger matrix element,

$$I(f,g)=\sum_k D(k)\begin{Bmatrix}l_1 & l_a & k\\ l_b & l_c & g\end{Bmatrix}+(-)^{f-g}\sum_k E(k)\begin{Bmatrix}l_1 & l_b & k\\ l_a & l_c & g\end{Bmatrix}, \tag{10}$$

with

$$D(k)=R_k(l_1,l_c,l_a,l_b)\begin{Bmatrix}l_1 & k & l_a\\ 0 & 0 & 0\end{Bmatrix}\begin{Bmatrix}l_c & k & l_b\\ 0 & 0 & 0\end{Bmatrix}, \tag{11}$$

$$E(k)=R_k(l_1,l_c,l_b,l_a)\begin{Bmatrix}l_1 & k & l_b\\ 0 & 0 & 0\end{Bmatrix}\begin{Bmatrix}l_c & k & l_a\\ 0 & 0 & 0\end{Bmatrix}, \tag{12}$$

and

$$R_k(l_1,l_c,l_a,l_b)=\int\int dr_1r_1^2dr_2r_2^2\varphi_1(r_1)\varphi_c(r_2)\left(\frac{r_<^k}{r_>^{k+1}}\right)$$
$$\times\varphi_a(r_1)\varphi_b(r_2) \tag{13}$$

(all in atomic units).

C. Results of the calculation

As in Refs. 6 and 7, we began by calculating $\alpha_{DR}(i,l_c\rightarrow d)$ for large numbers of intermediate states d using the angular momentum coupling-

independent approximation, Eqs. (6)–(9). We chose the initial states $i = 3s$ (ground state), $i = 3p$, and $i = 3d$. This was in keeping with the idea that, in low-density plasmas, radiative deexcitation proceeds much more rapidly than collisional excitation. Consequently, except for a possible Stark mixing of the $n = 3$ states, almost all Mo^{31+} ions are in their ground state. Results of these calculations were grouped according to type of single-particle excitation and appear in Tables I–V. The types of single-particle excitation are $2p \rightarrow n_a l_a$, $2s \rightarrow n_a l_a$, and $1s \rightarrow n_a l_a$ (all $\Delta n = n_a - n_1 \neq 0$), as well as $3s \rightarrow n_a l_a$ ($\Delta n \neq 0$ and $\Delta n = 0$), if $i = 3s$. Next, the $\alpha_{DR}(i, l_c \rightarrow d)$ values were summed over d and compiled, by excitation type, as $\alpha_{DR}(i, l_c)$. Finally, $\alpha_{DR}(i, l_c)$ was summed over l_c and compiled, by excitation type, as $\alpha_{DR}(i)$. All of these coupling-independent results appear in Sec. II.

Section III describes our calculations of $\alpha_{DR}(i, l_c \rightarrow d)$ and $\alpha_{DR}(i, l_c)$ in the L_{ab}, S_{ab} angular momentum coupling scheme. In this approach, the orbital and spin angular momenta of the pair of (Auger) active intermediate state electrons are held fixed while all other angular momenta are averaged. A DR rate coefficient was calculated for each choice of L_{ab} and S_{ab} allowed within an intermediate-state configuration. The total rate coefficient for that configuration is the sum of the rates computed for each value of L_{ab} and S_{ab}. In practice, only those intermediate states which made the largest contribution to the overall rate were given this more precise treatment. The average fractional change in the DR rate was determined for a collection of the most important intermediate states. The total coupling independent rate (obtained in Sec. II) was then reduced by this fraction to obtain the total DR rate coefficient, calculated in the L_{ab}, S_{ab} coupling scheme; see Fig. 3.

Section IV corrects the results of Sec. III for the effects of radiative cascade. Cascade corrected rate coefficients were calculated, in the L_{ab}, S_{ab} coupling scheme, for those intermediate states making the largest contribution to the overall rate. The average fractional change in the rate for these states was determined, and the total DR rate was then reduced by this fraction; see Fig. 3.

Section V collects our results in the form of a plot of $\alpha_{DR}(i)$ vs T (temperature) and summarizes our work. Throughout, values of α_{DR} are quoted in units of cm^3/sec.

II. COUPLING INDEPENDENT RESULTS ($T = 3$ keV)

In this section we report the results of our calculations of $\alpha_{DR}(i, l_c \rightarrow d)$ and $\alpha_{DR}(i, l_c)$ in the angular momentum fully averaged approximation. The relevant formulas for the Auger probability are those numbered (7)–(9). This is the simplest of the approximations which we considered. It has led in the past to values of $\alpha_{DR}(i)$ which may be too large[7] by up to a factor of 2.

Furthermore, results herein have not been corrected for the effects of radiative cascade; i.e., the radiative decay width $\Gamma_r(d)$ [Eq. (5)] includes contributions from all final states, whether or not they are stable to electron emission. This leads to an overestimation of the fluorescence yield [Eq. (2)] and to a further overestimation of the DR rate. Our calculations of the Auger widths $\Gamma_a(d)$ are, however, exhaustive. That is, for each intermediate state, all possible Auger decays $d \rightarrow i, l_c$ are considered and all Auger probabilities $A_a(d \rightarrow i, l_c)$ are computed.

A. $2p \rightarrow n_a l_a$ excitation

Table I contains a list of the dominant $\sum_{n_b} \alpha_{DR}(i, l_c \rightarrow d)$ values for each of the initial states $i = 3s$, $i = 3p$, and $i = 3d$. Asterisks label excitations which are not of the dominant $l_b = l_c - 1$, $l_a = l_1 + 1$ (pure dipole) type. The quoted DR rates have been summed over n_b ("n" in Table I). Within these sums, $\alpha_{DR}(i, l_c \rightarrow d)$ was not explicitly calculated if $n_b > 6$. Instead, for such cases Eq. (14) was used.[6]

$$\alpha_{DR}(i, l_c \rightarrow n_a, n_b) = (6/n_b)^3 \alpha_{DR}(i, l_c \rightarrow n_a, 6), \qquad (14)$$

TABLE I. $\sum_{n_b} \alpha_{DR}(i, l_c \rightarrow d)$ for $2p$ excitations; $i = 3s$, $3p$, and $3d$; $T = 3$ keV; coupling-independent results with no cascade correction, in units of cm^3/sec.

i	$\phi_a \phi_b$	l_c	$\sum_{n_b} \alpha_{DR}(i, l_c \rightarrow d)$
$3s$	$3dnd$	3	9.66×10^{-12}
	$3dnf$	4	3.54×10^{-12}
	$3pnd$	2*	2.66×10^{-12}
	$3dnp$ ($n > 3$)	2	1.49×10^{-12}
	$4dnd$ ($n > 3$)	3	1.27×10^{-12}
	$3dnd$	1*	9.31×10^{-13}
$3p$	$3dnd$	3	4.50×10^{-12}
	$3dnf$	4	2.02×10^{-12}
	$3pnd$	2*	9.86×10^{-13}
	$3dnp$ ($n > 3$)	2	7.35×10^{-13}
	$3dnd$	1*	4.67×10^{-13}
	$3dng$	5	1.85×10^{-13}
	$3pnp$ ($n > 3$)	1*	1.71×10^{-13}
$3d$	$3dnd$	3	4.47×10^{-12}
	$3pnd$	2*	2.47×10^{-12}
	$3pnp$	1*	1.60×10^{-12}
	$3dnf$	4	1.54×10^{-12}
	$3dnp$ ($n > 3$)	2	6.84×10^{-13}
	$3snp$	0*	4.73×10^{-13}
	$3dnd$	1*	4.28×10^{-13}

$$\sum_{l_a}\sum_{l_b}\sum_{n_b}\alpha_{DR}(i,l_c\to n_a,l_a,n_b,l_b)$$
$$=\left(\frac{5}{n_a}\right)^6\sum_{l_a}\sum_{l_b}\sum_{n_b}\alpha_{DR}(i,l_c\to 5,l_a,n_b,l_b). \quad (15)$$

For fixed i and l_c, $\alpha_{DR}(i,l_c\to d)$ was summed over d and a plot of $\alpha_{DR}(i,l_c)$ vs l_c, for fixed i, was obtained; see Fig. 1. Summing over d means summing over n_a, l_a, n_b, and l_b. Sums over n_b were performed first, as previously described. Sums over l_a and l_b were done next. For these, explicit calculations of $\alpha_{DR}(i,l_c\to d)$ were performed if l_a and $l_b<5$. Contributions from larger values of l_a and l_b were estimated.[10] Finally, the sum over n_a was approximated with the aid of Eq. (15). In all, $\alpha_{DR}(i,l_c\to d)$ values were computed for approximately 40 distinct intermediate states d for each of the three initial states i.

After summing the $\alpha_{DR}(i,l_c)$ values over l_c, total DR rate coefficients $\alpha_{DR}(i)$ for $2p$ excitation and for the initial states i are obtained. These are the following (in cm^3/sec):

$$\alpha_{DR}(i)=2.67\times10^{-11},\ i=3s$$
$$\alpha_{DR}(i)=1.27\times10^{-11},\ i=3p$$
$$\alpha_{DR}(i)=1.66\times10^{-11},\ i=3d.$$

The DR rate coefficients displayed in Table I sum to values which are 73%, 72%, and 70% of the total DR rate (for $2p$ excitation) for $i=3s$, $3p$, and $3d$, respectively. Additionally, one sees that the contribution of nondipole excitations amounts to 18% of the total DR rate (for $2p$ excitation) for both $i=3s$ and $3p$, and to 43% for $i=3d$.

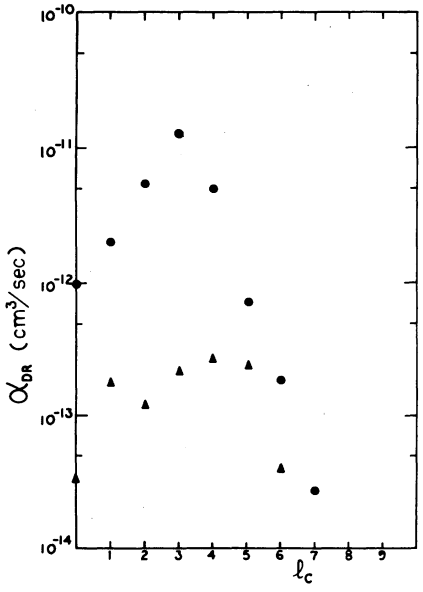

FIG. 1. $\alpha_{DR}(i,l_c)$ vs l_c for Mo^{31+}; $i=1s^22s^22p^63s$; coupling-independent result with no cascade correction: $2p$ excitations (●); $2s$ excitations (▲).

B. $2s\to n_al_a$ excitation

Table II contains a list of the dominant $\sum_{n_b}\alpha_{DR}(i,l_c\to d)$ values for each of the $n=3$ initial states. A plot of $\alpha_{DR}(i,l_c)$ vs l_c for fixed i can be found in Fig. 1. The manner in which these results have been obtained is described in Sec. II A.

After summing the $\alpha_{DR}(i,l_c)$ values over l_c, total DR rate coefficients $\alpha_{DR}(i)$ for $2s$ excitation and for the initial states i are obtained. These are the following (in cm^3/sec):

$$\alpha_{DR}(i)=1.1\times10^{-12},\ i=3s$$
$$\alpha_{DR}(i)=4.7\times10^{-12},\ i=3p$$
$$\alpha_{DR}(i)=1.9\times10^{-12},\ i=3d.$$

The DR rate coefficients displayed in Table II sum to values which are 53%, 58%, and 52% of the total DR rate (for $2s$ excitation) for $i=3s$, $3p$, and $3d$, respectively. Additionally, one sees that the contribution of nondipole excitations amounts to 52%, 83%, and 61% of the total DR rate (for $2s$ excitation) for $i=3s$, $3p$, and $3d$. This result makes suspect those calculations of α_{DR} which consider only dipole excitations.[8]

C. $1s\to n_al_a$ excitation

At 3 keV, $1s$ excitations make only very small contributions to the DR rate. The largest of these, for $i=3s$, are given in Table III.

After summing the $\alpha_{DR}(i,l_c)$ values over l_c, a total DR rate coefficient $\alpha_{DR}(i)$ for $1s$ excitation and $i=3s$ is obtained. This is

TABLE II. $\sum_{n_b}\alpha_{DR}(i,l_c\to d)$ for $2s$ excitations; $i=3s$, $3p$, and $3d$; $T=3$ keV; coupling-independent results with no cascade correction, in units of cm^3/sec.

i	$\phi_a\phi_b$	l_c	$\sum_{n_b}\alpha_{DR}(i,l_c\to d)$
$3s$	$3dnf$	5*	1.92×10^{-13}
	$3dnd$	4*	1.14×10^{-13}
	$3pnd$	3	1.09×10^{-13}
	$3pnf$	4	1.03×10^{-13}
	$3pns$ $(n>3)$	1	7.25×10^{-14}
$3p$	$3dnd$	4*	1.07×10^{-12}
	$3pnd$	3	4.70×10^{-13}
	$3snd$	2*	4.04×10^{-13}
	$3snp$	1*	3.42×10^{-13}
	$3dnp$ $(n>3)$	3*	2.11×10^{-13}
	$3dns$ $(n>3)$	2*	2.08×10^{-13}
$3d$	$3pnd$	3	2.38×10^{-13}
	$3dnf$	5*	2.25×10^{-13}
	$3snp$	1*	2.03×10^{-13}
	$3dnd$	4*	1.82×10^{-13}
	$3pns$ $(n>3)$	1	1.47×10^{-13}

TABLE III. $\sum_{n_b}\alpha_{DR}(i,l_c\to d)$ for $1s$ excitations; $i=3s$; $T=3$ keV; coupling-independent results with no cascade correction, in units of cm^3/sec.

i	$\phi_a\phi_b$	l_c	$\sum_{n_b}\alpha_{DR}(i,l_c\to d)$
$3s$	$3pnp$	2	3.49×10^{-16}
	$3pnd$	3	9.50×10^{-17}
	$3snp$	1*	6.15×10^{-17}
	$3pns$	1	4.39×10^{-17}
	$3pnp$	0*	3.53×10^{-17}
	$3dnp$ $(n>3)$	3*	3.36×10^{-17}

$$\alpha_{DR}(i)=8.4\times10^{-16},\ i=3s\ (cm^3/sec).$$

The DR rate coefficients displayed in Table III sum to a value which is 74% of the total DR rate (for $1s$ excitation). The contribution to the DR rate (for $1s$ excitation) made by nondipole excitations is 21%.

D. $3s\to n_a l_a$ excitation: $\Delta n\neq0$

Table IV contains a list of the dominant $\sum_{n_b}\alpha_{DR}(i,l_c\to d)$ values for $i=3s$. A plot of $\alpha_{DR}(i,l_c)$ vs l_c for $i=3s$ can be found in Fig. 2. The manner in which these results have been obtained is described in Sec. IIA. Sums over n_b begin with $n_b=5$. Explicit calculations of $\alpha_{DR}(i,l_c\to d)$ were performed for $n_b\leq7$. For $n_b>7$, $\alpha_{DR}(i,l_c\to d)$ was estimated.

After summing the $\alpha_{DR}(i,l_c)$ values over l_c, a total DR rate coefficient $\alpha_{DR}(i)$ is obtained. This is

$$\alpha_{DR}(i)=8.0\times10^{-12}\ (cm^3/sec).$$

The DR rate coefficients displayed in Table IV sum to a value which is 36% of the total DR rate (for $3s$, $\Delta n\neq0$ excitation). The contribution to the DR rate made by nondipole excitations is 100% (for $3s$, $\Delta n\neq0$ excitation).

TABLE IV. $\sum_{n_b}\alpha_{DR}(i,l_c\to d)$ for $3s$, $\Delta n\neq0$ excitations; $i=3s$; $T=3$ keV; coupling-independent results with no cascade correction, in units of cm^3/sec.

i	$\phi_a\phi_b$	l_c	$\sum_{n_b}\alpha_{DR}(i,l_c\to d)$
$3s$	$4snf$	3*	4.18×10^{-13}
	$4dng$	6*	3.71×10^{-13}
	$4dnh$	7*	3.22×10^{-13}
	$4fnd$	5*	3.06×10^{-13}
	$4sng$	4*	2.84×10^{-13}
	$4snd$	2*	2.80×10^{-13}
	$4fng$	5*	2.31×10^{-13}
	$4fns$	3*	1.89×10^{-13}
	$4fnh$	8*	1.76×10^{-13}
	$4fnh$	4*	1.64×10^{-13}

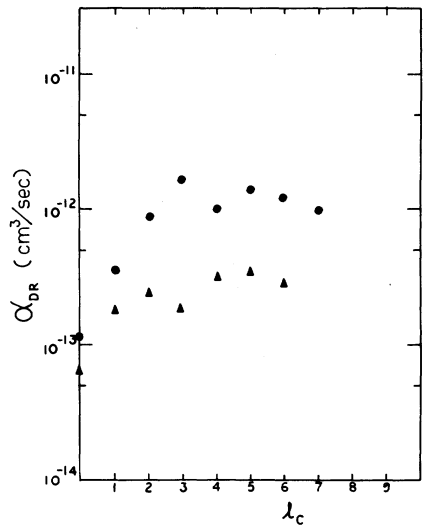

FIG. 2. $\alpha_{DR}(i,l_c)$ vs l_c for Mo^{31+}; $i=1s^2\,2s^2\,2p^6\,3s$; coupling-independent result with no cascade correction: $3s$, $\Delta n\neq0$ excitations (●); $3s$, $\Delta n=0$ excitations (▲).

E. $3s\to n_a l_a$ excitation: $\Delta n=0$

Table V contains a list of the dominant $\sum_{n_b}\alpha_{DR}(i,l_c\to d)$ values for $i=3s$. A plot of $\alpha_{DR}(i,l_c)$ vs l_c for $i=3s$ can be found in Fig. 2. The manner in which these results have been obtained is described in Sec. IIA. Sums over n_b begin with $n_b=13$ for $3s\to3p$ transitions, and with $n_b=9$ for $3s\to3d$ transitions. Only the first term in the sum was calculated explicitly; an analog of Eq. (14) was used to approximate higher terms.

After summing the $\alpha_{DR}(i,l_c)$ values over l_c, a total DR rate coefficient $\alpha_{DR}(i)$ is obtained. This is

TABLE V. $\sum_{n_b}\alpha_{DR}(i,l_c\to d)$ for $3s$, $\Delta n=0$ excitations; $i=3s$; $T=3$ keV; coupling-independent results with no cascade correction, in units of cm^3/sec.

i	$\phi_a\phi_b$	l_c	$\sum_{n_b}\alpha_{DR}(i,l_c\to d)$
$3s$	$3pnj$	8	2.58×10^{-13}
	$3pni$	7	2.57×10^{-13}
	$3pnh$	6	2.55×10^{-13}
	$3pnk$	9	2.40×10^{-13}
	$3png$	5	2.09×10^{-13}
	$3pnf$	2*	1.30×10^{-13}
	$3pnd$	1*	1.28×10^{-13}
	$3dng$	4*	1.49×10^{-13}
	$3dnf$	3*	1.43×10^{-13}
	$3dnh$	5*	9.4×10^{-14}
	$3dnd$	4*	9.1×10^{-14}
	$3dnd$	2*	4.8×10^{-14}
	$3dni$	8*	4.4×10^{-14}
	$3dni$	6*	4.0×10^{-14}

$\alpha_{DR}(i) = 3.2 \times 10^{-12}$ (cm^3/sec).

The DR rate coefficients displayed in Table V sum to a value which is 46% and 19% of the total DR rate (for $3s$, $\Delta n = 0$ excitation) for $\phi_a = 3p$ and $\phi_a = 3d$, respectively. The contribution to the DR rate made by nondipole excitations is 17% for $\phi_a = 3p$ and 100% for $\phi_a = 3d$ (for $3s$, $\Delta n = 0$ excitation).

III. L_{ab}, S_{ab} ANGULAR MOMENTUM COUPLING ($T = 3$ keV)

In the L_{ab}, S_{ab} coupling scheme the orbital and spin angular momenta of the excited electron pair are held fixed while all other angular momenta are averaged. An Auger probability is calculated for each of the allowed values of L_{ab} and S_{ab}, within an intermediate state configuration:

$$A_a(L_{ab}, S_{ab} | d \to i, l_c) = (2\pi/\tau)(0.5)(h_1 + 1)(2l_c + 1)(4l_a + 2 - h_a) \times (4l_b + 2 - h_b)(2l_a + 1)(2l_b + 1)\left|I(S_{ab}, L_{ab})\right|^2, \quad (16)$$

for $\varphi_a \neq \varphi_b$ and

$$A_a(L_{ab}, S_{ab} | d \to i, l_c) = (2\pi/\tau)(0.125)(h_1 + 1)(2l_c + 1)(4l_a + 2 - h_a) \times (4l_a + 1 - h_a)(2l_a + 1)^2\left|I(S_{ab}, L_{ab})\right|^2. \quad (17)$$

for $\varphi_a = \varphi_b$. Equations (16) and (17) may be derived from the fully angular momentum dependent Auger probability by averaging over the total orbital and spin angular momentum L and S of the intermediate state:

$$A_a(L_{ab}, S_{ab} | d \to i, l_c) = \frac{\sum_L \sum_S (2L+1)(2S+1) A_a(L, S, L_{ab}, S_{ab} | d \to i, l_c)}{\sum_L \sum_S (2L+1)(2S+1)}. \quad (18)$$

In general, the calculation of the Auger width $\Gamma_a(L_{ab}, S_{ab})$ must allow for the possibility of Auger decays into states other than the initial state; i.e., into a configuration of the target ion different from the initial configuration. Such decays can break the L_{ab}, S_{ab} coupling; e.g., the electron pair which decays may be different from the pair involved in excitation capture. For these decays, contributions to the Auger width were calculated in the coupling-independent scheme.

Although the radiative transition probability can depend upon L_{ab} and S_{ab}, the dominant cases were found to be independent of these quantum numbers. We made the approximation that $A_r(L_{ab}, S_{ab})$ was completely independent of L_{ab} and S_{ab}. Therefore, $A_r(L_{ab}, S_{ab})$ is given by Eq. (6).

The statistical weight of the intermediate state depends upon L_{ab} and S_{ab}, as

$$g_d(L_{ab}, S_{ab}) = (2L_{ab} + 1)(2S_{ab} + 1) g_d \text{ (spectators)}. \quad (19)$$

From Eqs. (1)–(6), (16), (17), and (19), a DR rate coefficient was calculated for each of the allowed values of L_{ab} and S_{ab} within a configuration. Table VI contains a list of the dominant $\sum_{n_b} \alpha_{DR}(i, l_c \to d | L_{ab}, S_{ab})$ values, for $i = 3s$ and $2p$ excitation. For pure dipole transitions the largest rate coefficient is associated with the largest allowed L_{ab} value. The corresponding $\sum_{L_{ab}} \sum_{S_{ab}} \sum_{n_b} \alpha_{DR}(i, l_c \to d | L_{ab}, S_{ab})$ values are also given. These should be compared with the results obtained in the angular momentum fully averaged approximation (Table I).

A list of the dominant $\sum_{n_b} \alpha_{DR}(i, l_c \to d | L_{ab}, S_{ab})$ values, for $i = 3s$ and for $3s$ excitation ($\Delta n \neq 0$), appears in Table VII. The corresponding $\sum_{L_{ab}} \sum_{S_{ab}} \sum_{n_b} \alpha_{DR}(i, l_c \to d | L_{ab}, S_{ab})$ values are also

TABLE VI. $\sum_{n_b} \alpha_{DR}(i, l_c \to d | L_{ab}, S_{ab})$ for the $2p$ excitations; $i = 3s$, $T = 3$ keV; L_{ab}, S_{ab} coupling results with no cascade correction, in units of cm^3/sec.

i	$\phi_a \phi_b$	l_c	L_{ab}	S_{ab}	$\sum_{n_b} \alpha_{DR}(i, l_c \to d \mid L_{ab}, S_{ab})$
$3s$	$3dnd$	3	4	0	3.07×10^{-12}
			3	1	2.73×10^{-12}
			2	0	8.12×10^{-13}
					...
					6.84×10^{-12}
	$3dnf$	4	5	0	1.23×10^{-12}
			5	1	8.56×10^{-13}
			4	1	5.86×10^{-13}
					...
					3.17×10^{-12}
	$3pnd$	2*	2	1	8.73×10^{-13}
			3	0	6.11×10^{-13}
			1	1	2.30×10^{-13}
					...
					2.08×10^{-12}
	$3dnp$ ($n > 3$)	2	3	0	5.40×10^{-13}
			2	1	4.71×10^{-13}
			1	0	1.39×10^{-13}
					...
					1.26×10^{-12}
	$4dnd$ ($n > 3$)	3	4	0	6.62×10^{-13}
			3	1	3.28×10^{-13}
			2	0	1.18×10^{-13}
					...
					1.11×10^{-12}
	$3dnd$	1*	1	1	4.68×10^{-13}
			2	0	2.40×10^{-13}
			0	0	2.30×10^{-13}
					...
					9.83×10^{-13}

TABLE VII. $\sum_{n_b}\alpha_{DR}(i,l_c\to d|L_{ab},S_{ab})$ for $3s$, $\Delta n\neq 0$ excitations; $i=3s$; $T=3$ keV; L_{ab},S_{ab} coupling results with no cascade correction, in units of cm^3/sec.

i	$\phi_a\phi_b$	l_c	L_{ab}	S_{ab}	$\sum_{n_b}\alpha_{DR}(i,l_c\to d\|L_{ab},S_{ab})$
$3s$	$4snf$	3*	3	1	2.19×10^{-13}
			3	0	7.40×10^{-14}
					2.93×10^{-13}
	$4dng$	6*	6	1	1.06×10^{-13}
			6	0	6.40×10^{-14}
					1.70×10^{-13}
	$4fns$	3*	3	0	8.90×10^{-14}
			3	1	2.20×10^{-14}
					1.11×10^{-13}
	$4fng$	5*	5	0	5.90×10^{-14}
			5	1	3.60×10^{-14}
					9.50×10^{-14}
	$4fnd$	5*	5	0	7.40×10^{-14}
			5	1	1.40×10^{-15}
					7.50×10^{-14}
	$4fng$	7*	7	1	3.50×10^{-14}
			7	0	1.70×10^{-14}
					5.20×10^{-14}

given. Compare these with the coupling independent results of Table IV. In the L_{ab},S_{ab} coupling scheme the total $\alpha_{DR}=2.6\times10^{-11}$ cm^3/sec.

IV. CASCADE CORRECTIONS ($T=3$ keV)

The form of the cascade corrections to the DR rate coefficients has been described in Ref. 7. The fluorescence yield $\omega(d)$ [our Eq. (2)] is modified to read

$$\omega(d)=\frac{1}{[\Gamma_r(d)+\Gamma_a(d)]}\times\left(\sum_{f'}(A_r(d\to f')+\sum_{d'}\frac{A_r(d\to d')A_r(d'\to f')}{[\Gamma_r(d')+\Gamma_a(d')]}+\cdots\right). \tag{20}$$

The states labeled f are stable against electron emission, whereas the states labeled d' are Auger unstable. The states labeled d can decay radiatively and/or by electron emission. Since most of the cascade decays are such as to break L_{ab}, S_{ab} coupling, cascade corrections to $\omega(d)$ were calculated entirely in the coupling independent scheme.

TABLE VIII. $\sum_{L_{ab}}\sum_{S_{ab}}\sum_{n_b}\alpha_{DR}(i,l_c\to d|L_{ab},S_{ab})$ for $2p$ excitations; $i=3s$; $T=3$ keV; L_{ab} coupling results with correction, in units of cm^3/sec.

i	$\phi_a\phi_b$	l_c	$\sum_{L_{ab}}\sum_{S_{ab}}\sum_{nb}\alpha_{DR}(i,l_c\to d\|L_{ab},S_{ab})$
$3s$	$3dnd$	3	6.34×10^{-12}
	$3dnf$	4	2.70×10^{-12}
	$3pnd$	2*	1.70×10^{-12}
	$3dnp$ $(n>3)$	2	1.22×10^{-12}

Table VIII contains a list of the dominant $\sum_{L_{ab}}\sum_{S_{ab}}\sum_{n_b}\alpha_{DR}(i,l_c\to d|L_{ab},S_{ab})$ values for $i=3s$ and $2p$ excitation which have been corrected for cascade. These results should be compared with the results of Tables VI and I.

V. SUMMARY

The coupling independent results of Sec. II are collected in Table IX; $\alpha_{DR}(i)$ values are listed according to initial state and target excitation type. For each of the three initial states, $2p$ excitations dominate the DR rate, amounting to 68%, 49%, and 59% of the total DR rate, for $i=3s$, $3p$, and $3d$, respectively. The $2s$ excitations make only a 3% and 7% contribution to the total DR rate for $i=3s$ and $3d$, but are 18% of the DR rate for $i=3p$. The increased contribution to DR made by $2s$ excitations, when $i=3p$, follows from an enhancement of the fluorescence yield by the radiative process $3p\to 2s+\gamma$. Similarly, the decreased contribution to the DR made by $2p$ excitations, when $i=3p$, is traced to the (dipole selection rule) suppression of the radiative process $3p\to 2p+\gamma$. The contribution of nondipole excitations to the DR rate is found to be 37%, 50%, and 64%, overall, for $i=3s$, $3p$, and $3d$, respectively. The preceding remarks refer to calculations for an electron temperature of 3 keV.

In Fig. 3 we plot values of $\alpha_{DR}(i)$ vs T (temperature) for $i=3s$ in the coupling independent (no cascade) and L_{ab}, S_{ab} coupling scheme with cascade correction included (———).

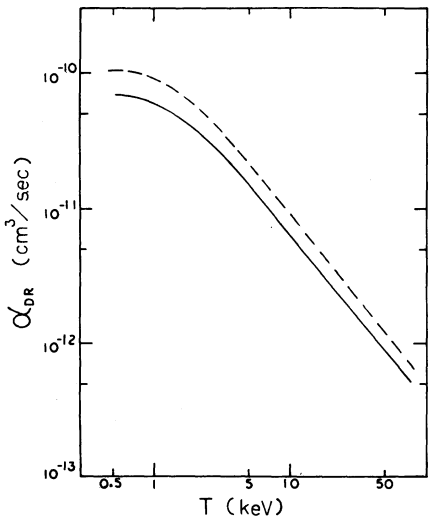

FIG. 3. $\alpha_{DR}(i)$ vs T (temperature); $i=1s^2\,2s^2\,2p^6\,3s$; all excitations: coupling-independent result with no cascade correction (---); L_{ab}, S_{ab} coupling result with cascade correction included (———).

TABLE IX. $\alpha_{DR}(i)$ for all excitations; $i=3s$, $3p$, and $3d$; $T=3$ keV; coupling-independent results with no cascade correction, in units of cm^3/sec.

$i=3s$	$i=3p$	$i=3d$
2.67×10^{-11} $(2p)$	1.27×10^{-11} $(2p)$	1.66×10^{-11} $(2p)$
1.1×10^{-12} $(2s)$	4.7×10^{-12} $(2s)$	1.9×10^{-12} $(2s)$
8.0×10^{-12} $(3s,\ \Delta n\neq0)$	6.6×10^{-12} $(3p,\ \Delta n\neq0)$	9.5×10^{-12} $(3d,\ \Delta n\neq0)$
3.2×10^{-12} $(3s,\ \Delta n=0)$	1.9×10^{-12} $(3p,\ \Delta n=0)$	
3.90×10^{-11}	2.59×10^{-11}	2.80×10^{-11}

cade corrections. As expected, the L_{ab}, S_{ab} coupling scheme reduces the DR rate below the values calculated in the coupling-independent approximation. The coupling-independent results themselves lie slightly above the corresponding values of α_{DR} calculated for the ion Mo^{32+}, at all temperatures.

The present result is the first calculation in which an open-shell ion is treated and should be useful in refining the existing phenomenological formula.[4,11,12] Extensions to other ions in the Na sequence will be presented as a sequel to this paper.[13]

Several important corrections have been neglected in this calculation which require further study; the configuration mixing effect should be quite important for the M-shell electrons, both in the initial and the intermediate states. Relativistic corrections are also expected to be sizable, especially for the $\Delta n=0$ excitations of the M shell. These effects, as well as the density effect, are being considered and will be discussed in more detail elsewhere.[14]

Note added in proof. Subsequently, we performed calculations of $\alpha_{DR}(i,l_c\rightarrow d)$ in a completely unaveraged L,S coupling scheme, considering only those intermediate states making the largest contribution to α_{DR}. Based upon these calculations, we expect a further reduction in the overall DR rate of ~15%, from the values obtained in the L_{ab},S_{ab} coupling scheme. Details of these more precise calculations are forthcoming.

ACKNOWLEDGMENTS

This work was supported by the U.S. Department of Energy under Contract No. DE-AC02-76. The numerical calculations were performed at the University of Connecticut Computer Center, which is supported, in part, by an NSF grant.

[1]J. N. Gau and Y. Hahn, J. Quant. Spectrosc. Radiat. Transfer 23, 121 (1980).
[2]E. Hinnov, Phys. Rev. A 14, 1533 (1976).
[3]A. Burgess, Astrophys. J. 139, 776 (1964).
[4]A. Burgess, Astrophys. J. 141, 1588 (1965).
[5]A. L. Merts, R. D. Cowan, and N. H. Magee, Jr., LASL Report No. LA-6220-MS, 1976 (unpublished).
[6]J. N. Gau, Y. Hahn, and J. A. Retter, J. Quant. Spectrosc. Radiat. Transfer 23, 131 (1980).
[7]J. N. Gau, Y. Hahn, and J. A. Retter, J. Quant. Spectrosc. Radiat. Transfer 23, 147 (1980).
[8]L. J. Roszman, Phys. Rev. A 20, 673 (1979).
[9]E. J. McGuire, in *Atomic Inner-Shell Processes*, edited by B. Crasemann (Academic, New York, 1975), Vol. I, pp. 296–309.
[10]J. N. Gau and Y. Hahn, Phys. Lett. 68A, 197 (1978).
[11]Y. Hahn, J. N. Gau, R. Luddy, and J. A. Retter, J. Quant. Spectrosc. Radiat. Transfer 23, 65 (1980).
[12]Y. Hahn, Phys. Rev. A 12, 895 (1975).
[13]K. LaGattuta and Y. Hahn (unpublished).
[14]K. LaGattuta and Y. Hahn (unpublished).